ELSEVIER

Physica A 306 (2002) 180–188

PHYSICA A

www.elsevier.com/locate/physa

Emergence of order in an oscillated granular layer

Daniel I. Goldman[a], M.D. Shattuck[a,1], Harry L. Swinney[a,*], Gemunu H. Gunaratne[b,c]

[a] *Center for Nonlinear Dynamics, The University of Texas at Austin, Austin, TX 78712, USA*
[b] *The Department of Physics, University of Houston, Houston, TX 77204, USA*
[c] *The Institute of Fundamental Studies, Kandy, Sri Lanka*

Abstract

Our experiments on a vertically oscillated granular layer reveal that spatial patterns emerge in two stages following a change of parameter into the pattern-forming regime: an initial, domain-forming stage and a later stage in which domains coarsen to form ultimately an extended regular pattern. We characterize the evolution of the pattern using a "disorder function" $\bar{\delta}(\beta)$, where β is a moment of the disorder operator (Gunaratne et al., Phys. Rev. E 57 (1998) 5146). The disorder in the initial stage is found to be consistent with a decay given by $\bar{\delta}(\beta) \sim t^{-\beta/2}$, in accord with theory that predicts that behavior in this stage should be universal for pattern forming systems. The final stage is non-universal.

PACS: 05.70.Ln; 82.40.Ck; 47.54.+r

Keywords: Pattern formation; Disorder; Granular media

1. Introduction

Nonequilibrium spatial patterns have been extensively studied in laboratory experiments and model systems, but most studies have focused on the dynamics of small deviations from asymptotic well-ordered states described by amplitude equations [1]. The dynamics of such perturbations exhibit universal (system-independent) properties.

* Corresponding author. Fax: +1-512-471-1558.
E-mail addresses: shattuck@ccny.edu (M.D. Shattuck), goldman@chaos.ph.utexas.edu, swinney@chaos.ph.utexas.edu (H.L. Swinney), gemunu@UH.edu (G.H. Gunaratne).
[1] Present address: Department of Physics, The City College of New York, New York, NY 10031, USA.

0378-4371/02/$ - see front matter
PII: S0378-4371(02)00496-X

Much less is understood about the development of a pattern from an arbitrary initial condition and the extent to which this dynamics is universal. We present experimental measurements of the time evolution (ordering) of a pattern from an initial noisy, featureless state and compare our observations to theory [2–6].

We characterize the development and ordering of a pattern using a recently introduced measure, the disorder function, $\bar{\delta}(\beta)$, which vanishes for any completely ordered pattern, and has a nonzero positive value that increases as the amount of disorder in the pattern increases. A further description of $\bar{\delta}(\beta)$ will be given in Section 4. Before presenting our main results, we describe our experimental apparatus in Section 2, present results for a typical experimental realization in Section 3, and review previous theoretical work on the development of nonequilibrium patterns in Section 4.

2. The experiment

Our experiments generate patterns in a layer of 0.165 mm bronze spheres contained in a vertically oscillated circular container with a diameter of 140 mm [7]. The layer is four particle diameters deep, and the cell is evacuated to 4 Pa so that hydrodynamic interaction between the grains and surrounding gas is negligible. The control parameters are the frequency f of the sinusoidal oscillations and the peak acceleration of the container relative to gravity, $\Gamma = (2\pi f)^2 A^2/g$, where A is the amplitude of the oscillation and g is the gravitational acceleration. As f and Γ are changed, a variety of temporally subharmonic patterns including locally square, striped, or hexagonal patterns are observed [7]. In this paper we consider the development of the square patterns.

To visualize patterns, the granular surface is illuminated with a ring of LEDs surrounding the cell and is strobed at the drive frequency of the container. The light is incident at low angles and the scattering intensity is a nonlinear function of the height of the layer; scattering from peaks (valleys) creates bright (dark) regions. The circular container allows relaxation to an almost perfect square array through wavelength adjustment of the pattern at the container wall over a distance of less than one wavelength[2]. In the region of the phase diagram studied, square patterns appear for increasing control parameter at $\Gamma \approx 2.75$; the bifurcation is subcritical. In our experiments, Γ is suddenly increased at a specific phase in the vibration cycle from an initial value of 2.2, where no discernible structure is observed. The grains are not in contact with the plate when the acceleration is changed, and we assume that the initiation of the quench (the time origin for our experiments) occurs at the last layer takeoff time before Γ is changed (the point where the acceleration of the plate is equal to $-g$); this is the lower bound of possible quench initiation times, and is physically reasonable, as it is the last time that the layer "knows" about the initial $\Gamma = 2.2$. The uncertainty in the time origin is the dominant source of systematic error in the interpretation of our observations.

[2] Experiments done in square containers also exhibit our main results. However, the formation of a single domain takes a much longer time, as the final pattern orientation is strongly influenced by the boundaries.

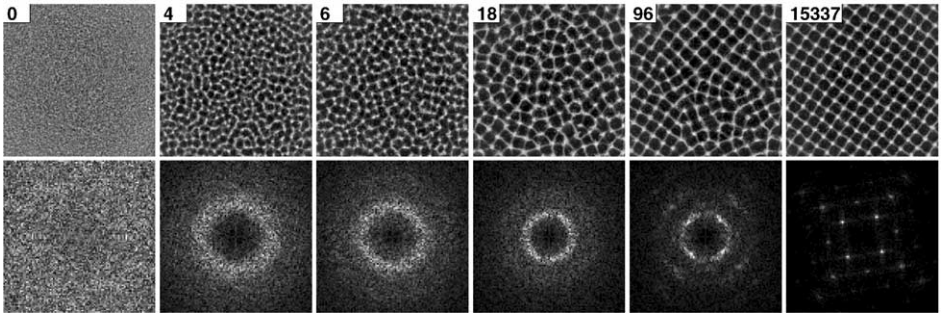

Fig. 1. Snapshots showing the emergence of a square spatial pattern in a granular layer at $f = 27$ Hz and $\Gamma = 3.3$; the times given in the upper left corner of each image are in units of container oscillation periods. Each image in the top row is of the central 8 cm of the 14 cm diameter circular container. Each image in the bottom row is the Fourier transform of the image above it. The first three frames of the top row show the emergence of local domains from a uniform background, and the last three show the slower coarsening of these domains to an almost perfect square array.

For a typical quench experiment, we take 10 sets of data at the same Γ and f, and record images of the pattern at a fixed phase in the oscillation cycle. Since the images' absolute phase in the oscillation cycle relative to the last layer takeoff time is arbitrary (chosen for highest contrast in the images), the time between the last layer takeoff time and the first image will not in general be an integer period of oscillation and may be different for different sets of runs, although this time is fixed within a set of 10 runs. Thus in our analysis of the image data, the values for the number of container oscillations may be fractional, but in each case there is one container oscillation between successive images (see the abscissas of Figs. 2 and 4; the number of periods has been rounded in Fig. 1).

3. Observations of the development of order

The emergence of local square domains and their coarsening to a final, almost perfect square array is shown in Fig. 1. The first three frames of the top row show that the system quickly (within six oscillations) creates a pattern with a range of orientational order the size of a wavelength. The last three frames show slow growth of domains of pattern with different orientations. These domains grow and compete, and the final state of the system is a single domain of pattern. This process can be viewed in Fourier space as well, as shown in the bottom row of Fig. 1. The early stage narrows the range of wave vectors in k-space, while the later stage selects a discrete set of wave vectors. We study aspects of this relaxation that are invariant under repetition of the experiment and analyze the dependence on the control parameters f and Γ. Our goal is to gain a quantitative understanding of the process of pattern evolution. Before we present our analysis of the observations, we review theoretical work on the evolution of patterns after a quench from an initial noisy and spatially featureless state and the methods that have been used to characterize this evolution.

4. Theory

Most analyses of the development of patterns have focused on solutions $u(\mathbf{x},t)$ to the Swift–Hohenberg equation [1],

$$\frac{\partial u}{\partial t} = (\varepsilon - (\triangle + k_0^2)^2)u - u^3 - v(\nabla u)^2 + \eta(\mathbf{x},t)\,, \tag{1}$$

where $u(\mathbf{x},t)$ is a two-dimensional scalar field, ε is the distance from pattern onset, v is the strength of a non-variational term [6], and η a random forcing term such that $\langle \eta(\mathbf{x},t)\eta(\mathbf{x}',t')\rangle = 2F\delta(\mathbf{x}-\mathbf{x}')\delta(t-t')$, where F denotes the strength of the noise. For suitable control parameters, random initial states evolve to patterns under spatiotemporal dynamics given by (1).

The most common measure used to characterize patterns generated by (1) is the width of the structure factor $S(t)$ [2–4,8] (i.e., the width of the peak in the azimuthal average of $\langle \tilde{u}(\mathbf{k},t)\tilde{u}(-\mathbf{k},t)\rangle$), which decays in two distinct stages [2]: $S(t) \sim t^{-1/2}$ is obeyed until the peak amplitude of the field $u(\mathbf{x},t)$ saturates, beyond which time the pattern coarsens and the decay becomes slower. For $\varepsilon = 0.25$ and $v = 0$, Elder et al. [3], Cross and Meiron [4], and Hou et al. [5] found that in this second region $S(t)$ decreased as $t^{-1/5}$ when $F = 0$, and as $t^{-1/4}$ when $F \neq 0$. Schober et al. [2] found that for $F = 0$ and $v = 0$, $S(t) \sim t^{-1/4}$; the discrepancy with earlier results could be due to the one-dimensionality of their model. [3]

The structure factor provides a single characterization of a pattern while the disorder function $\bar{\delta}(\beta)$ provides families of characterizations of a pattern, just as the generalized dimensions d_q [9] and singularity spectra $f(\alpha)$ [10] provide a family of characterizations of strange attractors. The details of a pattern depend on the initial state, but different patterns generated under fixed control parameters have the same $\bar{\delta}(\beta)$ [11]. For a pattern at fixed time represented by a scalar field $v(\mathbf{x})$ (e.g., $v(\mathbf{x}) = u(\mathbf{x},t_0)$ at time t_0) the disorder function is defined as

$$\bar{\delta}(\beta) = \frac{(2-\beta)}{(\int \mathrm{d}^2x)} \frac{\int \mathrm{d}^2x |(\triangle + k_0^2)v(\mathbf{x})|^\beta}{k_0^{2\beta}\langle |v(\mathbf{x})|\rangle^\beta}\,, \tag{2}$$

where k_0 is the typical wave vector associated with the pattern, $\langle |v(\mathbf{x})|\rangle$ denotes the mean of $|v(\mathbf{x})|$, $\bar{\delta}(\beta)$ $(0 \leqslant \beta < 2)$ has been normalized to be scale invariant, and $\int \mathrm{d}^2x$ is the area of the system. The ingredients used to deduce the form of the disorder function are its invariance under arbitrary rigid motions of the pattern and the fact that the pattern locally consists of a small number of plane waves. Modulation of squares due to curvature of the contour lines contributes to $\bar{\delta}(\beta)$ through the Laplacian, while variations of the size of squares contribute via the choice of a "global" k_0 [6]. Unlike the information contained in the structure factor, $|(\triangle + k_0^2)v(\mathbf{x})|$ is a measure of local irregularity in the pattern, and hence distinct "moments" β can be used to quantify

[3] Additional quantities have been measured in the second relaxation region. Hou et al. measured total domain wall length as a function of time. For $F = 0$, it was shown to decay as $t^{-1/4}$, while for $F \neq 0$ the decay was proportional to $t^{-0.3}$. Cross et al. showed that a stripe orientation correlation field decayed as $t^{-0.24}$. The interpretation of these results is that different measures probe different features of the pattern, and these features relax at different rates.

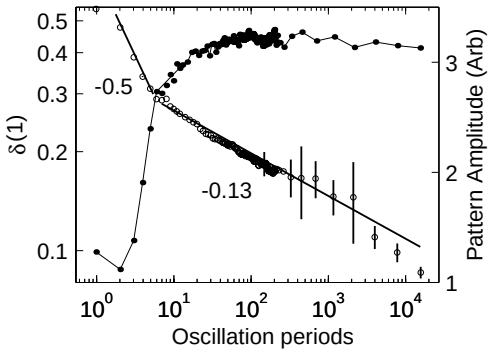

Fig. 2. The time evolution of the disorder function $\bar{\delta}(1)$ for square patterns at $\Gamma = 3.3$ (○), showing the domain forming stage with slope of -0.5 and the coarsening stage with slope of -0.13. Also shown is growth of the pattern amplitude (●), which grows rapidly in the domain-forming phase and saturates in the later coarsening phase. Each curve is an average of 10 runs at the same control parameters. The error bars at late times show typical variation between runs. The error bars at early times are the size of the symbols. The abscissa is in units of number of container oscillations from the last layer takeoff time before the container acceleration was changed.

multiple aspects of the disorder in patterns. For example, $\lim_{\beta\to 2}\bar{\delta}(\beta)$ is proportional to the density of defects [12].

Calculating $\bar{\delta}(\beta)$ for experimental data requires some care. Images shown in Fig. 1 have sharp changes at the edges which lead to high frequency contributions in their Fourier spectra. Consequently, their removal through simple filtering causes contamination of the pattern near the edges and leads to error in calculating the disorder function. We use a method of noise filtering that involves extending the image to a periodic one [13] using "Distributed Approximating Functionals" (DAFs) [14,15]. A method for calculating $\bar{\delta}(\beta)$ from filtered data has been presented in Ref. [11].

The disorder function analysis of the evolution of patterns generated by (1) from an initial noisy state reveals two stages: the emergence of domains characterized by $\bar{\delta}(\beta) \sim t^{-\sigma_E(\beta)}$, where $\sigma_E = \frac{1}{2}\beta$ is an exponent that characterizes this early stage, and a later slower domain-coarsening behavior characterized by $\bar{\delta}(\beta) \sim t^{-\sigma_L(\beta)}$ [6]. Unlike $\sigma_E(\beta)$, $\sigma_L(\beta)$ depends on the value of v in (1), and is thus expected to be system and model dependent. Since (1) contains the general features of a nonequilibrium pattern-forming system, we will compare the results obtained for $\bar{\delta}(\beta)$ from our experiments with the results from numerical simulations of (1) [6].

5. Analysis of the observations

5.1. Evolution of the disorder function for fixed Γ

The behavior of $\bar{\delta}(1)$ for the relaxation of Fig. 1 is shown in Fig. 2. In repetitions of the experiment for identical control parameters, the details of the patterns

differ for each run, but $\bar{\delta}(1)$ behaves the same. The initial formation of domains and the final coarsening exhibit different decay rates. The transition in behavior coincides with the saturation of the peak amplitude (cf. Fig. 2). This transition is consistent with that exhibited by the structure factor for the spatio-temporal dynamics of (1) [2].

During the initial stage of pattern formation the data are described by $\bar{\delta}(1) \sim t^{-0.5\pm0.1}$. The domain formation stage is short, lasting only through the first six periods of oscillation of the container; hence the observation of power law behavior in the initial stage is suggestive rather than conclusive. The uncertainty in the exponent is a result of two main sources of error. First, the short time range of the data makes the contribution of the beginning and end points of the initial region very important. The uncertainty in the time of the initiation of the quench contributes to a systematic shift in the value of the exponent; the value of -0.5 is found if we assume that the quench begins at the time of the last layer takeoff before Γ is changed (see discussion in Section 2). In addition, the end point of the initial region is known only to within one period of oscillation. Variation between runs also contributes to uncertainty in the exponent, but the error bars in Fig. 2 show that it is small relative to the above uncertainties.

Since nonlinear effects are negligible during the initial stage, the evolution can be modeled by (1) without nonlinear and stochastic terms. Numerical integration of noisy initial states shows that $\int \mathrm{d}^2x|u(\mathbf{x},t)| \sim \mathrm{e}^{\varepsilon t}t^{-1/4}$ and $\int \mathrm{d}^2x|(\triangle+k_0^2)u(\mathbf{x},t)| \sim \mathrm{e}^{\varepsilon t}t^{-3/4}$ [4]; consequently $\bar{\delta}(1) \sim t^{-1/2}$. The same behavior has been found in the initial decay of the structure factor [2] and in the rate of domain growth. More generally, for $0 < \beta < 2$, we find that in our data the moments of the disorder function decay as $\bar{\delta}(\beta) \sim t^{-\sigma_E(\beta)}$, where $\sigma_E(\beta) \approx \frac{1}{2}\beta$; see Fig. 3. This is also seen in numerical integration of the linearization of (1).

The latter stages of pattern formation correspond to nonlinear spatiotemporal dynamics of the field [2]. For the evolution shown in Fig. 2 at $\Gamma = 3.3$, the decay of disorder at long times is described by $\bar{\delta}(1) \sim t^{-0.13}$. This decay exponent is not expected to be universal [6]. The magnitude of the exponent is smaller than that for the relaxation rate of the structure factor upon integration of (1) with $F \neq 0$, -0.25 [3,5], and also with $F = 0$, -0.20 [3–5]. We find that $\sigma_L(\beta)$ is linear with $\sigma_L(\beta) \approx 0.13\beta$ (Fig. 3). In contrast, (1) yields [6] a nonlinear concave-down function for $\sigma_L(\beta)$. We speculate that the linearity found in our study implies that the spatiotemporal dynamics is governed by relaxation with a single length scale, and is thus a consequence of finite cell size. If we calculate $\sigma_L(\beta)$ for intermediate times (10–1000 oscillation periods), where domain sizes are small compared to the system size and boundary effects should be negligible, a nonlinear concave-down relationship is obtained. This nonlinearity implies that during intermediate times relaxation of the pattern occurs over multiple length scales, and work is in progress to test this hypothesis using (1).

[4] In the absence of diffusion, $u(\mathbf{x},t) \sim \mathrm{e}^{\varepsilon t}$. The effects of the diffusive terms are thus studied through the behavior of $\mathrm{e}^{-\varepsilon t}\int \mathrm{d}^2x|u(\mathbf{x},t)|$, which is numerically observed to decay as $t^{-1/4}$.

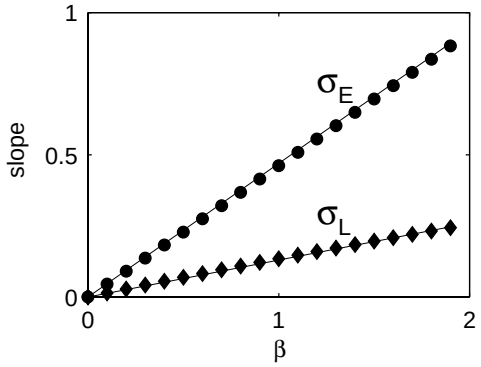

Fig. 3. The slopes of log–log plots of $\bar{\delta}(\beta)$ vs. β during domain formation (●) and domain coarsening (♦). The results are for a single run at $f = 27$ Hz and $\Gamma = 3.3$. There is no scatter in the curves because the calculation for $\bar{\delta}(\beta)$ is done for multiple values of β on the same data set. Since we assume that the quench initiation time is the time of last layer takeoff before the acceleration is changed, the uncertainty in the initial time does not enter the error calculation and the error estimates on the slopes of the lines, 0.47 ± 0.05 and 0.13 ± 0.02, are obtained by comparing different data sets within a 10 set run and different choices for the region over which a power law is fit. While statistical variation between runs is a source of error for both σ_E and σ_L, the narrow range of time in the first region is the dominant source of error for σ_E.

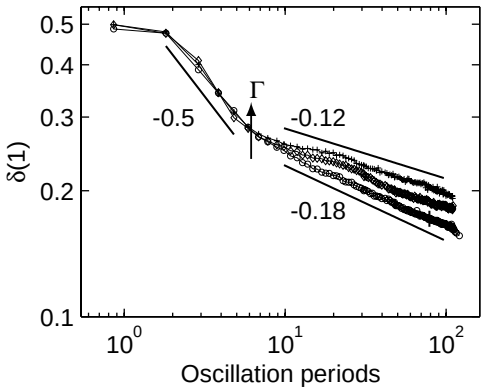

Fig. 4. The time evolution of $\bar{\delta}(1)$ for square patterns at three different final container accelerations, $\Gamma = 2.8$ (○), $\Gamma = 3.0$ (◇), and $\Gamma = 3.2$ (+). The decay during the initial domain forming stage is independent of Γ while the magnitude of the slope in the later stage decreases as Γ increases. The abscissa is in units of number of container oscillations from the last layer takeoff time before the container acceleration was changed.

5.2. Evolution of the disorder function for increasing Γ

Next, we consider changes in the behavior of the disorder function as Γ is increased from 2.8, driving the system further away from the onset of patterns (Fig. 4). We find that in the domain formation stage the exponent $\sigma_E(\beta)$ is independent of Γ; identical behavior is observed on integration of (1) [6]. Although the form of the curves in

the second region deviates from power law decay, the mean decay rate (measured by $\sigma_L(1)$ for a given Γ) decreases from 0.18 to 0.12 as Γ increases from 2.8 to 3.2; similar behavior is seen with decreasing v in (1) [6]. The long time behavior of the curves is not shown because for $\Gamma < 3.3$ a secondary oscillatory motion dominates the dynamics of the pattern after about 100 oscillations; work is in progress to understand these oscillatory dynamics.

6. Conclusions

We have shown that the formation of a pattern in a vertically oscillated granular layer occurs in two distinct stages. During the early stage the spatiotemporal dynamics is essentially linear and the decay of the disorder function determined in our experiment is consistent with the power law found in pattern formation for the Swift–Hohenberg equation: $\bar{\delta}(\beta) \sim t^{-\sigma_E(\beta)}$, with $\sigma_E(\beta) \simeq \frac{1}{2}\beta$. During the later domain coarsening stage the emergence of order is described by $\bar{\delta}(\beta) \sim t^{-\sigma_L(\beta)}$, where $\sigma_L(\beta)$ is a nonlinear function at intermediate times and becomes linear at long times, when the finite system size dominates the decay. This relaxation is not universal, since the decay rate (and thus $\sigma_L(1)$) decreases with increasing Γ. Such behavior is also seen in model systems, in which $\sigma_L(\beta)$ is a model and parameter dependent nonlinear function of β [6]. Such characterizations of pattern formation can be used to determine the validity and limitations of model systems [16], and can be used to study patterns and their evolution in other laboratory experiments.

Acknowledgements

We have benefited from discussions with M. Golubitsky, J.B. Swift, and P. Umbanhowar. The research at the University of Texas was supported by the Engineering Research Program of the Office of Basic Energy Sciences of the U.S. Department of Energy. Additional support came from the Office of Naval Research (GHG), and the National Science Foundation (GHG).

References

[1] M.C. Cross, P.C. Hohenberg, Rev. Mod. Phys. 65 (1993) 851.
[2] H.R. Schober, E. Allroth, K. Schroeder, H. Müller-Krumbhaar, Phys. Rev. A 33 (1986) 567.
[3] K.R. Elder, J. Viñals, M. Grant, Phys. Rev. A 46 (1992) 7618.
[4] M.C. Cross, D.I. Meiron, Phys. Rev. Lett. 75 (1995) 2152.
[5] Q. Hou, S. Sasa, N. Goldenfeld, Physica A 239 (1997) 219.
[6] G.H. Gunaratne, A. Ratnaweera, K. Tennekone, Phys. Rev. E 59 (1999) 5058.
[7] F. Melo, P.B. Umbanhowar, H.L. Swinney, Phys. Rev. Lett. 75 (1995) 3838.
[8] J.J. Christensen, A.J. Bray, Phys. Rev. E 58 (1998) 5364.
[9] H.G.E. Hentschel, I. Procaccia, Physica 8D (1983) 835.
[10] T.C. Halsey, M.H. Jensen, L.P. Kadanoff, I. Procaccia, B.I. Shraiman, Phys. Rev. A 33 (1986) 1141.
[11] G.H. Gunaratne, D.K. Hoffman, D.J. Kouri, Phys. Rev. E 57 (1998) 5146.

[12] G.H. Gunaratne, R.E. Jones, Q. Ouyang, H.L. Swinney, Phys. Rev. Lett. 75 (1995) 3281.
[13] D.K. Hoffman, G.H. Gunaratne, D.S. Zhang, D.J. Kouri, Chaos 10 (2000) 240.
[14] D.K. Hoffman, M. Arnold, D.J. Kouri, J. Phys. Chem. 96 (1992) 6539.
[15] D.K. Hoffman, D.J. Kouri, Proceedings of the Third International Conference on Mathematical and Numerical Aspects of Wave Prop. Phenom., SIAM, 1995, pp. 56–83.
[16] For example, S.C. Venkataramani, E. Ott, Phys. Rev. Lett. 80 (1998) 3495.